Microsystem Technologies 7 (2001) 183–187 © Springer-Verlag 2001

Micro materials modeling in MINIMOS-NT

V. Palankovski, S. Selberherr

Abstract Considerable effort was spent on our two-dimensional device simulator MINIMOS-NT to get it ready for simulation of devices with high complexity in respect to materials, geometries, etc. Many of the existing physical models (band gap, mobility, thermal conductivity, energy relaxation times, specific heat, etc.) were refined, some of them were replaced by promising new ones, and many new models were added as well. Being an ancestor of the well-known MOS device simulator MINIMOS [1], its experience with Si devices was inherited. Thereby, MINIMOS-NT became a generic device simulator accounting for a variety of micro-materials, including group IV semiconductors, III-V compound semiconductors and their alloys, and non-ideal dielectrics.

1
Introduction

Several applications of industrial interest employ devices operating in a wide temperature range. Therefore, our models have been designed to meet this challenge in addition to the conventional silica applications. MINIMOS-NT has been successfully used for simulation of heterostructure devices, e.g. high electron mobility transistors (HEMTs) and heterojunction bipolar transistors (HBTs) [2, 3]. Physics-based DC-simulation, mixed-mode device/circuit simulation, small signal RF-parameter simulation, and device reliability investigations of high practical value were performed.

2
Sets of partial differential equations

In MINIMOS-NT carrier transport can be treated by the drift–diffusion (DD) and the hydrodynamic (HD) transport models. In addition, the lattice temperature can be treated either as a constant or as an unknown governed by the lattice heat flow equation, thus, self-heating (SH) effects are accounted for.

V. Palankovski (✉), S. Selberherr
Institute for Microelectronics,
TU Vienna Gusshausstrasse 27–29,
A-1040 Vienna, Austria
E-mail: vassil.palankovski@iue.tuwien.ac.at

This work is supported by Infineon Technologies AG, Munich, Germany.

3
Modeling of the materials properties

One of the strong features of MINIMOS-NT as a generic device simulator is its capability to consider various semiconductor materials, such as III-V binary and ternary compounds, and SiGe. The past modeling experience from Si MOS structures [4] and $Al_{0.2}$ $Ga_{0.8}$ As/$In_{0.2}$ $Ga_{0.8}$ As/GaAs HEMTs [5] is inherited and preserved.

A large number of published theoretical and experimental reports have been reviewed to include the physical parameters for the Si, Ge from chemical group IV, and GaAs, AlAs, InAs, InP, or GaP, which are III-V chemical group binary compounds. All these materials are named *basic materials* later in this work. The combination between two III-V binary materials results in a ternary or a quaternary material. SiGe as a combination of Si and Ge, together with the ternary III-V materials as a combination of the respective binary materials are named alloy materials later in this work. An attempt has been made to allow the user choose arbitrary mole fractions for the alloy materials, although the majority of the simulations performed in this work include III-V compounds lattice-matched to GaAs substrate. This not only gives the designer a good degree of freedom as to the choice of material, but also allows a direct comparison between various devices such as AlGaAs/GaAs, InGaP/GaAs, InP/InGaAs, InAlAs/InGaAs, and SiGe/Si HBTs, AlGaAs/InGaAs/GaAs and InAlAs/InGaAs HEMTs, or SiGe/Si MOSFETs. However, due to the very limited experimental data on some compound materials such as InGaP, InAlAs, InAsP, and GaAsP, one has to consider interpolation schemes as the only available option to model the variation of some parameters in a continuous range of mole fraction. In these cases, variations of interpolation schemes are studied to find the best fit to the sometimes limited reported data in the literature.

For all models in MINIMOS-NT the general modeling approach is to employ universal models, i.e. the same functional form to be used for all materials, just with different parameter sets. In models for alloy materials the respective models for the two basic materials are employed first and then combined as a function of the material composition x. Additionally, full consistency between the alloy materials and the basic materials is obtained by having all the models for alloy materials inheriting their model parameters from the models for basic materials. Although it is arbitrary which of the two basic materials will correspond to a mole fraction $x = 0$ and which to a

mole fraction $x = 1$, a choice has to be done, e.g. InGaAs is used for $In_xGa_{1-x}As$ and not for $In_{1-x}Ga_xAs$.

Material parameters of Si, Ge, GaAs, InP, GaP, InAs, and InGaAs, as well as to some extent SiGe and AlGaAs, have received considerable attention in the past and many experimental data and theoretical studies for these parameters can be found in the literature. On the other hand, the band structure and transport related parameters of other III-V ternary and all quaternary materials has been the topic of few or no experimental/theoretical publications. These facts necessitate the use of some interpolation scheme, essentially based on known values of the physical parameters for the related basic materials and alloy materials. In the cases when experimental data scatters the most consistent or most recent published data has been adopted. In the cases when experimental data is inconsistent or missing Monte-Carlo (MC) simulation has been considered. Although the interpolation scheme is still open to experimental or MC verifications, it provides more useful and reliable material parameters for numerical device simulation over the entire range of alloy composition.

For many parameters, such as various lattice parameters, a linear interpolation is sufficient. Some parameters, like the electronic bandgap exhibit a strong non-linearity with respect to the alloy composition which arises from the effects of alloy disorder. In such cases, a quadratic interpolation is used and a so-called bowing parameter is introduced. For other parameters, such as carrier mobility, a linear interpolation of the inverse values – Mathiessen rule is used. Finally, there are parameters, such as thermal conductivity, for which none of the interpolation schemes mentioned so far is sufficient, and a quadratic interpolation of the inverse values together with an inverse bowing factor is proposed. The choice of interpolation formula largely depends on factors such as required accuracy, the physical nature of the parameter, and available experimental or MC data.

3.1 Thermal modeling for SH

The coefficients of the lattice heat flow equation are the mass density, specific heat, and thermal conductivity of the respective materials. A linear interpolation between the values of the mass density of the basic materials is assumed for alloy materials. The temperature dependence of the thermal conductivity is modeled by a simple power law which gives a good agreement with experimental data [6]. A harmonic mean is taken to model the material composition dependence of the thermal conductivity in the case of alloy materials. The lattice temperature dependence of the specific heat capacity is computed by a new model suggested in [7].

3.2 Carrier mobility

Electron and hole mobilities are among the most important carrier transport parameters. They are basic inputs for expressing the current in the semiconductor materials. The carrier mobilities are influenced by several physical mechanisms, such as scattering by interaction with thermal lattice vibrations, charged or neutral impurities, lattice defects, and surfaces. For alloy materials also alloy scattering mechanism has to be accounted for. The mobility models have to support both the DD and the HD transport models. While the low-field mobility is independent of the transport model used, the high-field mobility is modeled in a different way. Thus, the various effects affecting the mobility are grouped into low-field effects, including the impact of lattice scattering, ionized impurities scattering, and surface scattering, and high-field effects, respectively.

For Si the established mobility model of MINIMOS 6 [8] is used. The approach is extended for all other semiconductor materials. A model which distinguishes between the majority and minority electrons, as well as between dopant species is described in [9]. The temperature dependence of the lattice mobility preserves the expression from the mobility model of MINIMOS 6. The mobility reduction due to ionized impurity scattering is accounted for by temperature dependent parameters. The model is applicable to any material of interest (e.g. see Fig. 1). The results delivered by the model for the hole mobility as a function of the doping concentration for various III-V group binary semiconductors compared to measured data are shown in Fig. 2.

Mobility reduction due to a high field is modeled for DD equations. For HD equations the deviation from the ohmic low-field mobility is modeled as a function of the carrier temperature after Hänsch et al. [10]. The energy relaxation times and the saturation velocities are modeled separately.

In the case of alloy materials the model employs the low-field mobilities of the basic materials and combines them by a harmonic mean. The respective interpolations are also done in the models for the saturation velocities and, in the case of HD simulation, of the energy relaxation times. The models are based on experimental or Monte-Carlo simulation data and employ analytical functional forms which cover the whole material composition range. The energy relaxation times are used in the HD mobility models, in the energy balance equations of the hydrodynamic transport model, and in the lattice heat flow equa-

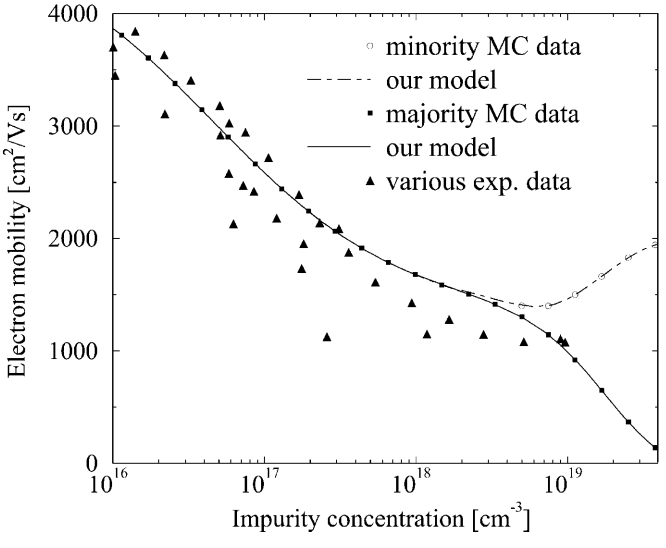

Fig. 1. Electron mobility in InP at 300 K. Our analytical model is compared to MC simulation data and experimental data

tion. The energy relaxation times for electrons depend on the lattice temperature and on the carrier temperature [11].

3.3
Bandgap energy, bandgap offsets, and bandgap narrowing

The bandgap (or forbidden energy zone) is one of the most important semiconductor parameters. Various models define the temperature dependence of the bandgap energy in semiconductors (e.g. [12]). For alloys the temperature-dependent bandgaps of the constituents are calculated first. The bandgap and the energy offset are then calculated depending on the material composition. This is important to assure consistency between the values for alloy materials at $x = 0$ and $x = 1$ and the values for the respective basic materials. For materials where the bandgap changes between direct and indirect the multiple valley conduction bands are considered.

The problem to align the bandgaps of two or more different materials is old and not completely solved [13, 14] due to the dependence on the growth conditions. The many suggested approaches mainly differ in whether to use the electron affinity to align the conduction bands, whether to align the midgaps, or whether to align the valence band edges. In MINIMOS-NT the last approach is used. An energy offset is used to align the band edge energies of different materials. It has an arbitrary value and by changing it consistently for all materials at the same time the same results are obtained. As a default in MINIMOS-NT for the group IV materials the reference material is Si. The origin of the energy axis is assumed to be in the middle of the Si bandgap at 300 K. For the III-V material system GaAs is chosen as the reference material. The change of the bandgap with the material composition of alloy materials is defined by the ratio $\Delta E_C/\Delta E_g$. For example, for $Al_xGa_{1-x}As$/GaAs interface it is known that this ratio equals 60%. This means that, with increasing x, 60% of the increase of the bandgap ($\Delta E_g = \Delta E_C + \Delta E_V$) is contributed to the conduction band (ΔE_C) and 40% to the valence band (ΔE_V). Using the default model parameters in MINIMOS-NT ratios $\Delta E_C/\Delta E_g$ of 0.12 for SiGe, 0.6 for AlGaAs, 0.5 for InAlAs, 0.6 for InGaAs, InAsP, GaAsP, and 0.3 for InGaP are obtained, which are in fairly good agreement with experimental data. The complete bandgap alignment of all semiconductor materials presented in MINIMOS-NT is shown in Fig. 3.

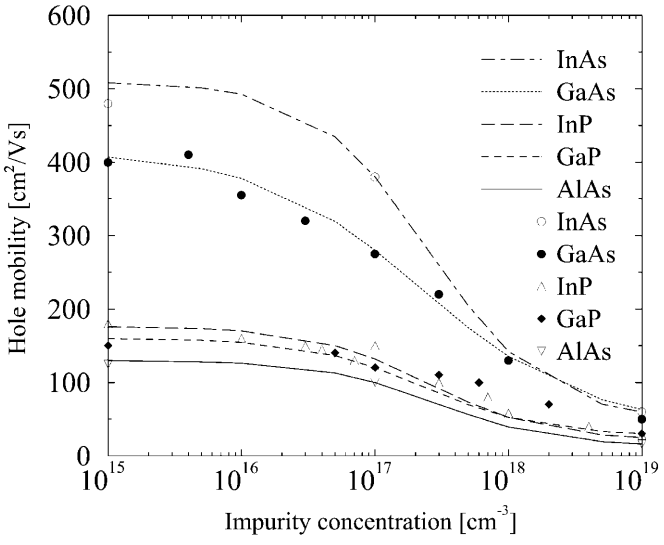

Fig. 2. Hole mobility vs. doping concentration at 300 K. Comparison between the model and experimental data

In previous work we emphasized on bandgap narrowing as one of the crucial heavy-doping effects to be considered for bipolar devices [15]. We have developed a new physically-based analytical bandgap narrowing model applicable to compound semiconductors, which accounts for the semiconductor material, the dopant species, and the lattice temperature.

3.4
Effective carrier masses and effective density of states

In MINIMOS-NT parabolic conduction and valence bands are assumed, and the effects of band non-parabolicity are assumed to be negligible. Therefore, effective masses for each of the three conduction band minima (Γ, X, and L) can be defined and used to calculate the density of states (DOS). The effective DOS masses scaled by the free elec-

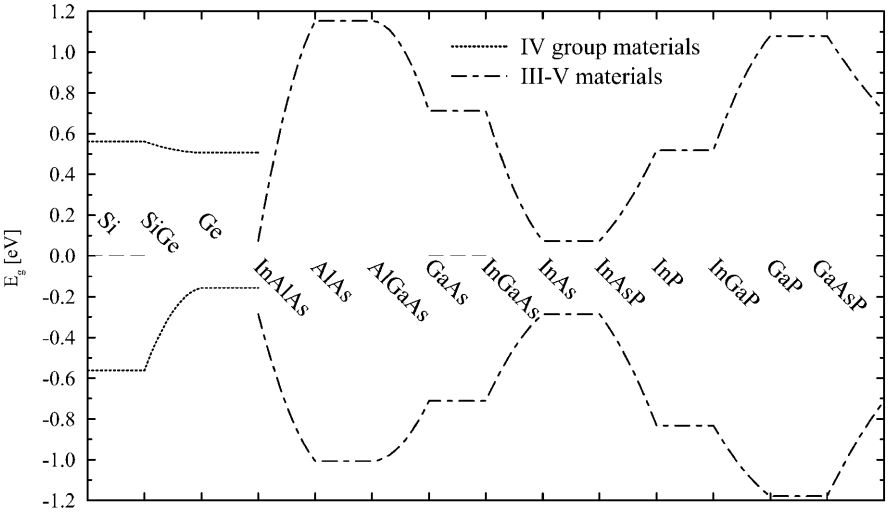

Fig. 3. Bandgaps of all semiconductor materials modeled in MINIMOS-NT: reference energies for IV group and III-V group materials are the mid gaps of Si and GaAs, respectively, placed at 0 eV

tron mass give relative carrier masses. In materials with direct bandgap the value of the relative mass for electrons from the Γ valley is considered. In the case of materials with indirect bandgaps namely Si, Ge, AlAs, and GaP the transverse and the longitude electron masses from the X valley (respectively L valley for Ge) are taken into account. For all materials the hole masses account for heavy and light hole masses. A linear temperature and a quadratic temperature dependence are used in the case of electrons and holes, respectively. For alloy materials the temperature dependence is introduced first. Then a quadratic interpolation of the masses is used as a function of the material composition.

The model for the DOS represents a theoretical expression which takes into account the number of equivalent energy minima. In case of a transition between a direct and indirect bandgap, the valley degeneracy factor is modeled accordingly.

3.5 Generation and recombination

Carrier generation in space charge regions and recombination in e.g. high injection regions is modeled using the well known Shockley–Read–Hall (SRH) equation. A trap assisted band-to-band tunneling model (BBT) describes the generation of carriers in high field regions. The model modifies the SRH lifetimes by field enhancement factors. Surface recombination is accounted for by a model which modifies the SRH lifetimes depending on the carrier surface recombination velocities and the surface distance. The Auger-processes are modeled using a triple concentration product. The processes are the inverse processes to the impact ionization process. The direct BBT model describes the carrier generation in high field regions without any influence of local traps. The type of the impact ionization model depends on the used equation set. Using the DD equation set, an electric field dependent model is used to calculate the generation rate. In HD simulations the carrier temperatures are solved together with the carrier concentrations and the potential. The information about the carrier temperatures is used for the hydrodynamic impact ionization model.

3.6 Interface models

The device geometry is partitioned into independent regions, so-called segments. For these segments different sets of parameters, models and algorithms can be defined independently. The segments are linked together by interface models which account for the interface conditions. The interface models for the carrier concentrations specify the solution for the continuity equations with the unknown concentration quantities on the device segments. To calculate the carrier concentrations and the carrier temperatures at the interface of two semiconductor segments three different models are implemented in MINIMOS-NT. These are a model with continuous quasi-Fermi level across the interface (CQFL), the thermionic emission model (TE), and the thermionic field emission model (TFE). The derivation of these models is described in [16]. By using the CQFL model a Dirichlet interface condition is applied. The carrier concentrations are directly determined in a way that the quasi-Fermi level across the interface remains continuous. The model is suitable for use at homojunctions. The TE model is commonly used to model the current across heterojunctions of compound semiconductors. The TFE model extends the TE model by accounting for tunneling effects through the heterojunction barrier by introducing a field dependent barrier height lowering.

4 Simulation results

Several types of HBTs have been analyzed to obtain one concise set of model parameters, used in all simulations. For example, in Fig. 4 we present the simulated forward Gummel plot for an AlGaAs/GaAs HBT compared to experimental data. The simulation results at 373 K demonstrate the ability of MINIMOS-NT to reproduce correctly the thermal device behavior. Furthermore, very good agreement also for the reverse Gummel plots has been achieved, e.g. in Fig. 5 the comparison with measured data for InGaP/GaAs HBT is shown.

5 Summary

Several sophisticated models have been created and employed to get good agreement with experimental results, and also to aid getting an insight and understanding of the real device and thus achieve better device performance. For example, in [17] simulation results for several different types of GaAs-based and Si-based HBTs demonstrating the extended capabilities of MINIMOS-NT are shown, most of them in comparison with experimental data. Two-dimensional DC-simulations of four different types of one-finger devices in very good agreement with measured data in a wide temperature range are demonstrated. Self-heating effects are accounted for the output device characteristics. The work is extended with transient simulation of small-

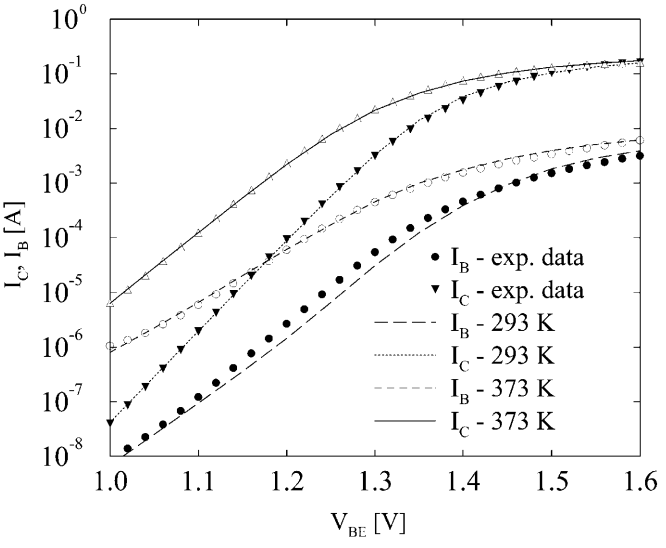

Fig. 4. Forward Gummel plots at $V_{CB} = 0$ V. Comparison with measured data at 293 and 373 K

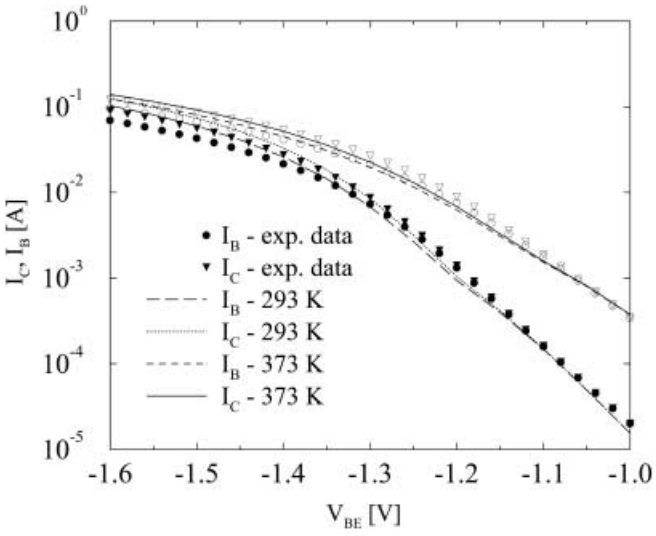

Fig. 5. Reverse Gummel plots at $V_{CB} = 0$ V. Comparison with measured data at 293 and 373 K

signal parameters to connect DC- and RF-operation. Device reliability investigations which confirm the usefulness of device simulation for practical applications are also offered.

References

1. **Selberherr S; Schütz A; Pötzl H** (1980) MINIMOS – a two-dimensional MOS transistor analyzer. IEEE Trans. Electron Devices ED-27 (8): 1540–1550
2. **Quay R; Reuter R; Palankovski V; Selberherr S** (1998) S-parameter simulation of RF-HEMTs. In: Proc High Performance Electron Devices for Microwave and Optoelectronic Applications EDMO, Manchester, UK, pp. 13–18
3. **Palankovski V; Selberherr S; Schultheis R** (1999) Simulation of heterojunction bipolar transistors on Gallium-Arsenide. In: Proc Intl Conf on Simulation of Semiconductor Processes and Devices, Kyoto, Japan, pp. 227–230
4. **Grasser T; Tsuneno K; Masuda H; Selberherr S** (1998) Mobility parameter tuning for device simulation. In: Touboul A; Danto Y; Klein J.-P; Grünbacher H; (eds) 28th European Solid-State Device Research Conference (Editions Frontiers) Bordeaux, France, pp. 336–339
5. **Simlinger T; Brech H; Grave T; Selberherr S** (1997) Simulation of submicron double-heterojunction high electron mobility transistors with MINIMOS-NT. IEEE Trans. Electron Devices 44 (5): 700–707
6. **Maycock P** (1967) Thermal conductivity of silicon, germanium, III-V compounds and III-V alloys. Solid-State Electron 10: 161–168
7. **Palankovski V; Selberherr S** (1999) Thermal models for semiconductor device simulation. In: IEEE Proc Third European Conference on High Temperature Electronics, Berlin, Germany, pp. 25–28
8. **Selberherr S; Hänsch W; Seavey M; Slotboom J** (1990) The evolution of the MINIMOS mobility model. Solid-State Electron 33 (11): 1425–1436
9. **Palankovski V; Kaiblinger-Grujin G; Selberherr S** (1998) Implications of dopant-dependent low-field mobility and band gap narrowing on the bipolar device performance. J Phys IV 8: 91–94
10. **Hänsch W; Orlowski M; Weber W** (1988) The hot-electron problem in submicron MOSFET. In: Nougier J.-P; Gasquet D (eds) 18th European Solid State Device Research Conference Montpellier, France, J. Phys, 49: 597–606 (les éditions de physique)
11. **Gonzales B; Palankovski V; Kosina H; Hernandez A; Selberherr S** (1999) An energy relaxation time model for device simulation. Solid-State Electron 43: 1791–1795
12. **Varshni Y** (1967) Temperature dependence of the energy gap in semiconductors. Physica 34: 149–154
13. **Capasso F; Margaritondo G** (eds) (1987) Heterojunction Band Discontinuities. Elsevier, North Holland Physics Publishing, Elsevier, Amsterdam
14. **Van de Walle C** (1989) Band lineups and deformation potentials in the model-solid theory. Physical Review B 39 (3): 1871–1883
15. **Palankovski V; Kaiblinger-Grujin G; Selberherr S** (1999) Study of dopant-dependent band gap narrowing in compound semiconductor devices. Materials Science and Engineering B66: 46–49
16. **Simlinger T** (1996) Simulation von Heterostruktur-Feldeffekttransistoren. Dissertation, Technische Universität Wien, http://www.iue.tuwien.ac.at/phd/simlinger
17. **Palankovski V** (2000) Simulation of Heterojunction Bipolar Transistors. Dissertation, Technische Universität Wien, http://www.iue.tuwien.ac.at/phd/palankovski